Mechatronics and Automation Technology
J. Xu (Ed.)

doi:10.3233/ATDE221215

Appointed-Time Control for Euler-Lagrange Systems with Perturbations

Haiqing XING[a], Zhengshu MA[a], Lei SUN[a], Xiaohua SONG[a], Bin FANG[a], Caiguo MA[a], Xiaoyu XIONG[a] and Jundong LIU[b,1]

[a] *STATE GRID Hangzhou Yuhang Power Supply Company, Hangzhou 310000, China.*

[b] *School of Automation, Hangzhou Dianzi University, Hangzhou 310018, China.*

Abstract. In this paper, a time-varying controller is developed for Euler-Lagrange systems with bounded disturbances. A mapping strategy is designed to make the convergence time of the system achieve at an arbitrarily pre-assigned finite time. The selection of the time period is independent of the initial conditions, and the performances is free of chattering. To be specific, the proposed controller is constructed in two steps: Firstly, a common PD controller is designed to ensure the asymptotical stability of the nominal system; Secondly, by employing the mapping strategy, then the obtained new controller can make the disturbed system converged at a specified time. In the simulations, a two-link manipulator is used to validate that both uniformly stability for the undisturbed system and pre-assigned time attraction for the disturbed system can be achieved.

Keywords. Euler-Lagrange systems, appointed-time control, mechanical arm, time-varying control.

1. Introduction

1.1. Research Background and Significance

With the rapid development of economy and science and technology, a variety of new and high technologies are emerging in modern society. A new round of technological industrial revolution is booming, which is bound to make the industry more dependent on automation and information means to improve their industrial competitiveness and economic benefits.

Therefore, more and more industries choose to introduce manipulator systems to help people complete tasks. Especially in the power industry, when carrying the high-voltage live working, there always exist complexity and diversity of live working objects, relatively complex working environment and high potential safety hazards, people must constantly develop safer and more efficient live working methods, which brings good market prospects for the development of high-voltage live working robots [1].

Live working is an important method to test, repair and transform power equipment. It has made great contributions to improving power supply reliability, reducing power outage losses, and ensuring power grid safety [2]. Traditional manual live working

[1] Corresponding Author, Jundong LIU, School of Automation, Hangzhou Dianzi University, Hangzhou 310018, China; E-mail: liujundong@hdu.edu.cn.

requires workers to use a variety of insulated hot rods or insulated gloves to contact the high-voltage line indirectly/directly in an insulated bucket raised to the height. Therefore, workers are always in a very dangerous working environment. Manual live line work requires very strict safety protection and shielding. If the workers' pay little attention, they will directly face the risk of electric shock. When working on overhead transmission lines, the workers are in a high-altitude environment, which increases the risk of falling from high altitude. In addition, traditional live line operation often requires the cooperation of many skilled workers, and the technical requirements of workers are relatively high.

In order to overcome the difficulties and deficiencies of manual live line operation and meet people's demand for continuous power supply. It is very necessary to develop a live working robot system with stronger safety and adaptability, overcome the difficulties and limitations of manual live working, and replace manual live working, and meet the actual time requirements in real applications [3].

1.2. Research Status

In recent years, with the rapid update and development of cooperative manipulator products, and with the popularization of applications in various industries, cooperative manipulators have gradually received extensive attention. Therefore, more and more scientists have invested in the research of cooperative control of manipulators. Up to now, fruitful achievements have been obtained. When applying the multi-manipulator consensus theory to engineering practice, its application objects are mostly nonlinear systems. Among them, Euler-Lagrange system is a classical and universal nonlinear system, and the form of Euler-Lagrange equation is often used to describe the manipulator model. Specifically, the existing results on cooperative control of manipulator are mainly divided into the following aspects.

Convergence performance: Note from [4] that the convergence of coordinated control objectives for multiple Euler-Lagrange systems can be achieved within a fixed time, which is independent of initial conditions. Based on the Lyapunov stability and the nearest neighbor-interactions rules, the fixed-time bipartite consensus problem for Euler-Lagrange systems with a directed signed communication network was investigated in [5] by using a distributed estimation-based control protocol. In [6], the authors proposed a new distributed fast non-singular terminal sliding mode controller to study distributed finite-time containment control problem for multi-agent systems with double-integrator leaders and Euler-Lagrange followers.

Model independence: The problem of model-independent distributed containment control for multiple Euler-Lagrange systems with external disturbances and uncertainties was studied in [7]. In [8], a new model-independent distributed control approach was presented for cooperative formation tracking of multiple Euler-Lagrange systems.

Time delay: In [9], a new event-triggered communication scheme for Euler-Lagrange systems with communication time delays was presented.

Collision avoidance/obstacle avoidance: By integrating an improved distributed optimization algorithm and an adaptive control law, the authors achieved distributed optimal formation for uncertain Euler-Lagrange systems with collision avoidance in [10]. In [11], a novel log-type attractive potential field was utilized to achieve the obstacle avoiding task and trajectory tracking task of uncertain Euler-Lagrange systems.

1.3. Purpose of This Article

Although there are many new achievements in the research of mechanical arm, it is still not enough to replace manual work at heights with mechanical arm. And it can be seen from [12] to [15] that in recent years, the research on aerial live working robots mostly focuses on the safety and structural design of the robot itself, the positioning of the work target and remote-control methods. In general, the live working process can be roughly divided into three processes: grabbing the branch line, transporting the branch line near the main line, and clamping the main line and the branch line. The completion time for each task of the manipulators should be designed at specific finite time, otherwise, the operation efficiency will greatly reduce. Therefore, the research on the time optimization of high-altitude live working robot has very important practical significance.

2. Problem Formulation

2.1. Problem Statement

An illustration of the high altitude live working robot is given in figure 1, where labels ① to ⑥ represent insulated bucket arm, live wire, mechanical arm end tool, mobile lifting platform, mechanical arm, mobile lifting platform and operating platform, respectively. Then the live working process can be roughly divided into three processes (shown in figure 2): grabbing the branch line, transporting the branch line near the main line, and clamping the main line and the branch line.

In this paper, we set the whole process time as t, specify the designated location as Q_1, the process time of grasping the branch line as t_1, the process time of transporting the branch line to Q_1 as t_2, and the process time of clamping the main line and branch line as t_3. Each time is limited, and the mapping strategy and obstacle avoidance method are adopted, so that the operation originally required a long time can be completed within a specified time. Thus, the operation time of the whole process can be shortened finally.

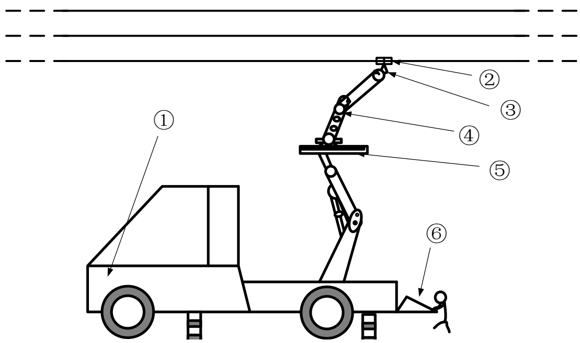

Figure 1. Schematic diagram of live working

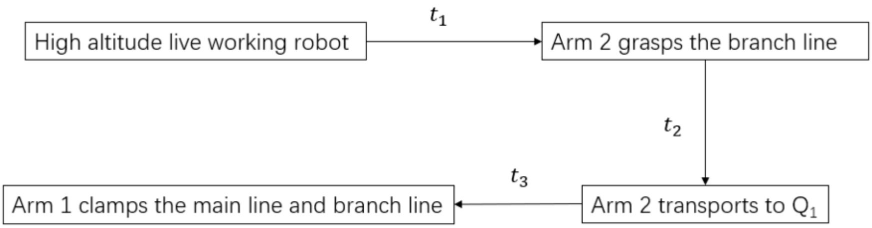

Figure 2. Flow chart of live working

Consider the Euler-Lagrange system described as follows:

$$M(q_i)\ddot{q}_i + C(\dot{q}_i, q_i)\dot{q}_i + g(q_i) = u_i, i = 1,2 \tag{1}$$

where $q_i \in R^n$ and $u_i \in R^n$ are the system state variable and the control input vector, respectively. $M(.): R^n \to M^n$ represents the inertia matrix, $C(.,.): R^n \times R^n \to M^n$ represents the centripetal-Coriolis matrix. The inertia matrix $M(q_i)$ is positive-definite, the centripetal-Coriolis matrix $C(\dot{q}_i, q_i)$ is linear in $\dot{q}_i$, and $\dot{M}(q_i) - 2C(\dot{q}_i, q_i)$ is skew-symmetric.

A perturbation signal $d(t)$: $[0, \infty) \to R^n$ added to equation (1) can be described as follows:

$$M(q_i)\ddot{q}_i + C(\dot{q}_i, q_i)\dot{q}_i + g(q_i) = d(t) + u_i, i = 1,2 \tag{2}$$

where the disturbance $d(t)$ denotes unknown bounded external disturbance and its upper bound is unknown.

Assumption 1: Assume that the disturbance signal $d(t)$ is bounded within any finite time interval, i.e., for every $\tau > 0$, there exists a positive constant $\bar{d} > 0$ such that $||d(t)|| < \bar{d}$ for all $t \in [0, \tau)$, where $\bar{d}$ can be unknown.

2.2. Mapping Strategy

This section mainly introduces some content about mapping strategies.

Definition 1: The following definitions will be used in the follow-up developments.

1) A continuous function $y(.): [0, \tau) \to [0, \infty)$ belongs to class Y(or $y \in Y(\tau)$) if it is strictly increasing subject to $lim_{t \to 0^+} y(t) = 0$ and $lim_{t \to \tau^-} y(t) = \infty$.

2) $y(t) \in Y$ belongs to class $Y_1 \subset Y$ if there exist $\dot{y}(0) = 1$ and $\ddot{y}(t) \geq 0$ for all $t \in [0, \tau)$.

3) A continuous function $z(.): [0, \infty) \to [0, \tau)$ belongs to class Z(or $z \in Z(\tau)$), suppose that its inverse function satisfies $z^{-1} \in Z(\tau)$. Then, it yields that z is a continuous increasing function to $lim_{t \to 0^+} z(t) = 0$ and $lim_{t \to \infty} z(t) = \tau$.

4) $z(t) \in Z$ belongs to class $Z_1 \subset Z$ if there exist $\dot{z}(0) = 1$ and $\ddot{z}(t) < 0$ for all $t \in [0, \infty)$.

According to the above definitions and reference [16], one can obtained the following results directly.

Lemma 1: $\dot{z}(t) := dz(t)/dt$, $\ddot{z}(t) := d^2z(t)/dt^2$, $y'(z(t)) := dy(z)/dz$ and $y''(z(t)) := d^2y(z)/dz^2$.Then, the following statements will hold for any functions $y \in Y(\tau)$ and $z = y^{-1} \in Z(\tau)$.

1) $\dot{z}(t) = 1/y'(z(t))$ and $y''(z(t))\dot{z}^2(t) + y'(z(t))\ddot{z}(t) = 0$.

2) $y'(.): [0, \tau) \to [0, \infty)$, $y''(.): [0, \tau) \to R$, $lim_{t\to\tau^-}\, y'(t) = lim_{t\to\infty}\, y''(t) = \infty$.

3) $\dot{z}(.): [0, \infty) \to [0, \infty)$, $\ddot{z}(.): [0, \infty) \to R$, $lim_{t\to\infty}\, \dot{z}(t) = -lim_{t\to\infty}\, \ddot{z}(t) = 0$.

4) Suppose that $Y_3 = Y_1 + Y_2$ and Y_1, Y_2 are class Y functions, then it yields that Y_3 belongs to class Y as well. Similarly, it follows from $Z_3 = Z_1 + Z_2$ and Z_1, Z_2 belong to class Z that $Z_3/2$ also belongs to class Z.

5) If $\alpha \geq 1$, $\dot{z}^{\alpha}(t)$ will be the derivative of a class Z function.

6) For $\alpha > 0$, function $\beta e^{-\alpha t}$ can be regarded as the derivative of a class $Z(\tau)$ function if and only if there holds $\beta = \alpha\tau$.

Assumption 2: Let t_0 denote the initial time and $\Delta t_j = t_j - t_0$, $j = 1,2,3$. Suppose that there exist $z_i \in Z(t_j)$ and $\tilde{t}_j > t_0$ such that for any $t_j > 0$ the closed-loop response of system (1) under infinite-time control $u_i = f(\dot{q}_i, q_i)$ satisfies $\|\dot{q}_i(t_j)\| \leq \dot{z}_i(\Delta t_j)$ for all $t \in [\tilde{t}_j, \infty)$ and any of the following conditions is met:

1) $\|\ddot{q}_i(t_j)\| \leq \dot{z}_i{}^2(\Delta t_j), \forall t \in [\tilde{t}_j, \infty)$.

2) $\|f(\dot{q}_i, q_i)\| \leq \dot{z}_i{}^2(\Delta t_j), \forall t \in [\tilde{t}_j, \infty)$.

With the above preparations, some main results are provided in the following section.

3. Main Results

Theorem 1 (Nominal system): Suppose that $y \in Y_1(\tau)$ and $z \in Z_1(\tau)$ are symmetric about $y = x$, and $h(\dot{q}, q, t)$ is designed as follows:

$$h(\dot{q}, q, t) = \begin{cases} \dot{y}^2(\Delta t) f(\dot{q}/\dot{y}(\Delta t), q) + [\ddot{y}(\Delta t)/\dot{y}(\Delta t)]M(q)\dot{q} \\ +[1 - \dot{y}^2(\Delta t)]g(q), t \in [t_0, t_0 + \tau) \\ \qquad f(\dot{q}, q), t \in [t_0 + \tau, \infty) \end{cases} \tag{3}$$

Then, the closed-loop system modeled by the Euler-Lagrange equation (1) and the prescribed-time control $u = h(\dot{q}, q, t)$ is (globally) uniformly prescribed-time stable and converges at $t = t_0 + \tau$, if system (1) under the controller $u = f(\dot{q}, q)$ can exponentially converge to 0 with any initial state and y satisfies：

$$y(\Delta t) = \tau[1 - exp(-\alpha\Delta t/||X||)] \tag{4}$$

where $\alpha \in (0, 0.5)$, $X \in M^n$ and satisfies the following equation:

$$XQ + Q^T X = -I_n \tag{5}$$

with $Q \in M^n$and Q satisfies:

$$||\,exp(Qt)|| \leq \sqrt{2||X^{-1}||||X||}\, exp(-t/(2||X||)) \tag{6}$$

Proof: The mapped part of system (1) by replacing with q and t, then one can obtains

$$M(q)\ddot{q} + C(\dot{q},q)\dot{q} + \dot{y}^2(\Delta t)g(q) - \frac{\ddot{y}(\Delta t)}{\dot{y}(\Delta t)}M(q)\dot{q} = \dot{y}^2(\Delta t)f(\dot{q}/\dot{y}(\Delta t),q) \quad (7)$$

Note that the relationship between equation (7) and system (1) is one-to-one mapping of an attractive infinite-time closed loop solution. In the following, we will explore a control input $u = h(\dot{q},q,t)$ for system (1) such that its closed-loop system performs similar behaviors to those of equation (7). With these discussions, the goal can be achieved by using (3) for $t \in [t_0, t_0 + \tau)$ with a simple substitution.

In the following, we will discuss adding perturbed to the system of Theorem 1.

Theorem 2 (Perturbed system): During the Step 1, Step 2 and Step 3, set $t_0 = 0$ and select the qualified $d(t)$. Besides, we construct that $y \in Y_1(t_j)$ is the inverse function of $z_i \in Z(t_j)$ and function $h^j(\dot{q}_i, \tilde{q}_i, t_j)$ is shown by this:

$$h^j(\dot{q}_i,\tilde{q}_i,t_j)\begin{cases}\dot{y}^2(\Delta t_j)f(\dot{q}_i/\dot{y}(\Delta t_j),\tilde{q}_i) + [\ddot{y}(\Delta t_j)/\dot{y}(\Delta t_j)]M(q_i)\dot{q}_i \\ +\left[1-\dot{y}^2(\Delta t_j)\right]g(q_i), t_j \in [t_0, t_0+\tau), i = 1,2, j = 1,2,3 \\ \quad f(\dot{q}_i,\tilde{q}_i), t_j \in [t_0+\tau,\infty), i = 1,2, j = 1,2,3\end{cases} \quad (8)$$

If system (1) is globally prescribed-time tracking by using $u_i = h^j(\dot{q}_i, q_i, t_j)$, then the perturbed system (2) will be globally prescribed-time attractive and co nverge at $t = t_j$ with the prescribed-time control $u_i = h^j(\dot{q}_i, \tilde{q}_i, t_j)$.

In Step 1, map system (2) onto a finite interval, then the closed-loop form of system (2) with $u_1 = f(\dot{q}_1, q_1, t_1)$ can be given as follows:

$$M(q_1)\ddot{q}_1 + C(\dot{q}_1,q_1)\dot{q}_1 + \dot{y}^2(t_1)g(q_1) - \frac{\ddot{y}(t_1)}{\dot{y}(t_1)}M(q_1)\dot{q}_1$$

$$= d(t) + \dot{y}^2(t_1)f(\dot{q}_1/\dot{y}(t_1), q_1) \quad (9)$$

Note that the above equation is acquired by using the mapping strategy similar to system (7). With the above developments, one can construct a $u_1 = h^1(\dot{q}_1, q_1, t_1)$ for system (2) such that the closed-loop system performs similar behaviors to (9). Then we can achieve the goal by a simple substitution and the use of (8) for $t \in [t_0, t_0 + t_1)$.

In addition, by using the reverse-mapping of (9):

$$M(q)\ddot{q} + C(\dot{q},q)\dot{q} + g(q) = f(\dot{q},q) + \dot{z}^2 d(z(t)) \quad (10)$$

where $\dot{z}^2 d(z(t))$ tends to 0 when $t \to \infty$ since $d(t)$ satisfies Assumption 1. Thus, system (2) under the infinite-time control exhibits same behaviors to the closed-loop of system (1).

In Step 2 and Step 3, the corresponding detailed analyses are the same as above, which are omitted for space limitation.

Remark 1: For t_j, it satisfies $t_1 + t_2 + t_3 \le \tau$, which τ represents the limited time of the whole operation process. It is equivalent to setting the working time periods of Step 1, Step 2 and Step 3 within t_1 t_2 and t_3, respectively, such that the time of whole operation process within τ.

4. Simulation

4.1. Mapping Functions

Three Y class functions can be constructed as follows with $a_i > 0$, $b_i > 0$ and $c_i > 0$:

$$y(t) = \sum_{i=1}^{n} a_i t^{b_i}/(\tau - t)^{c_i} \tag{11}$$

$$y(t) = -\sum_{i=1}^{n} a_i \, ln(1 - t/\tau) \tag{12}$$

$$y(t) = \sum_{i=1}^{n} a_i \, tan^{b_i}(\pi t/2\tau) \tag{13}$$

In the following simulations, set $a_i = 20$, $b_i = 1$, $c_i = 1$, $\tau = 20 \text{ and } 30$ for comparisons.

4.2. Two-link Manipulators

Consider a two-link robotic manipulator with the following dynamics:

$$\begin{bmatrix} M_{11} & M_{12} \\ M_{21} & M_{22} \end{bmatrix} \begin{bmatrix} \ddot{q}_1 \\ \ddot{q}_2 \end{bmatrix} + \begin{bmatrix} C_{11} & C_{12} \\ C_{21} & C_{22} \end{bmatrix} \begin{bmatrix} \dot{q}_1 \\ \dot{q}_2 \end{bmatrix} + G(q) = u \tag{14}$$

where the dynamics parameters for each manipulator are as follow:

$$M_{11}(q) = 8cos(q_2) + 13 \tag{15}$$

$$M_{12}(q) = M_{21}(q) = 4\,sin(q_1 + q_2)\,sin(q_1)$$
$$+2\,sin^2(q_1 + q_2) + 0.5 \tag{16}$$

$$M_{22}(q) = 2\,sin^2(q_1 + q_2) + 0.5 \tag{17}$$

$$C_{11} = -8cos(q_1 + q_2)\dot{q}_2 \tag{18}$$

$$C_{12} = -8cos(q_1 + q_2)(\dot{q}_1 + \dot{q}_2) \tag{19}$$

$$C_{21} = 8cos(q_1 + q_2)\dot{q}_1 \tag{20}$$

$$C_{22} = 0 \tag{21}$$

$$G(q) = \begin{bmatrix} g(6\,cos(q_1) + 2\,cos(q_1 + q_2)) \\ g(2\,cos(q_1 + q_2)) \end{bmatrix} \tag{22}$$

where the parameters of the 2-DOF manipulator are shown in table 1:

Table 1. The parameters of the 2-DOF manipulator

	the length of links	the center of mass positions	the mass of the links	the moments of inertia
Arm 2	$l_1 = 2m$	$l_{c1} = 1m$	$m_1 = 2kg$	$I_1 = 0.5kg \cdot m^2$
Arm 1	$l_2 = 2m$	$l_{c2} = 1m$	$m_2 = 2kg$	$I_2 = 0.5kg \cdot m^2$

Set the initial state variables $q = \dot{q} = 0,\ t_0 = 0$ and the gravitational acceleration $g = 9.81m/s^2$. In addition, the desired position to be reached is $q_d = [90^o \quad 0]^T$.

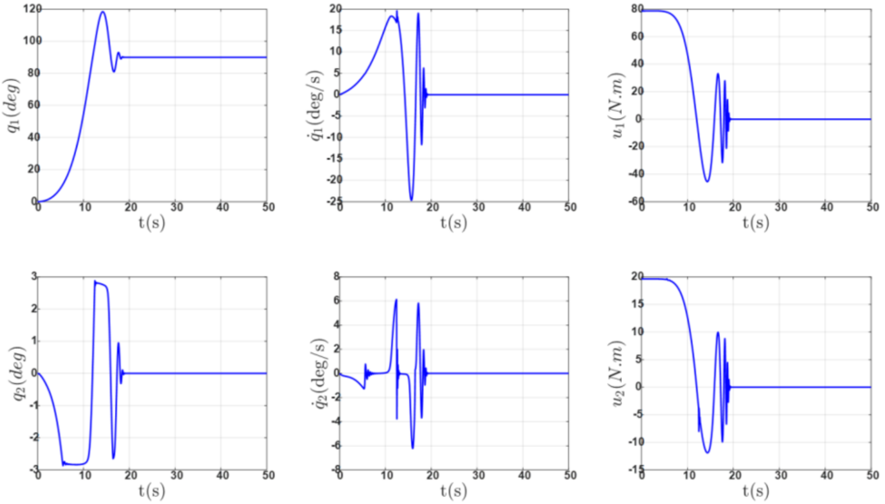

Figure 3. The state trajectories under PD controller with $a_i = 20,\ b_i = 1,\ c_i = 1,\ \tau = 20$.

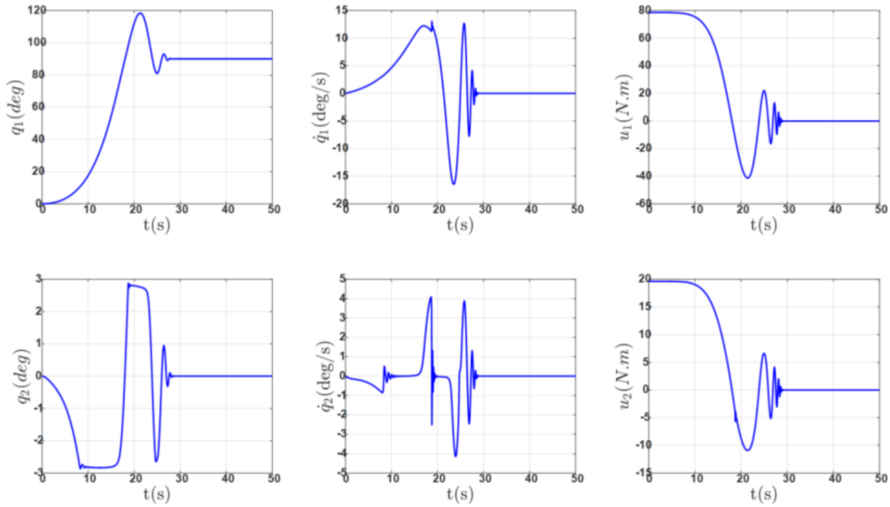

Figure 4. The state trajectories under PD controller with $a_i = 20,\ b_i = 1,\ c_i = 1,\ \tau = 30$.

It can be seen from figure 3 and figure 4 that the manipulator can achieve the goals in both cases, where the convergence time in figure 3 is before 20s, while 30s in figure 4. This indicates that the proposed preassigned-time control law performs well. In addition, it can be found that the fluctuation and the peak value of $\dot{q}$ and $\dot{u}$ in figure 4 are obviously smaller than those in figure 3 when the evolution of time approaches to the specific time instant 20s and 30s, respectively. Hence, there always exist tradeoffs between the performance and the convergence time.

5. Conclusions

This paper mainly introduced a prescribed-time controller. On the basis of infinite-time controller, a novel preassigned-time controller was developed by using a mapping strategy. It is found that the smaller the specified convergence time, the greater the fluctuation of its acceleration and control torque when it is close to convergence time instant.

References

[1] Zhao Y. Research on computer virtual simulation system of high-voltage charged robot[J]. Wireless Internet Technology, 2012, (6): 96-96.
[2] Li J, Lu S, Wang Z. Development of live working robot for 220kV substation[J]. Manufacturing Automation, 2013, 35(17) : 76-79, 2013.
[3] .Zhao Y, Lu S, Lv C. Design of hydraulic mechanical arm with force feedback for charged repair robot[J]. Hydraulic and pneumatic, 2013, (8): 31-34.
[4] Xu T, Z. Duan, Sun Z and Chen G. "Distributed fixed-time coordination control for networked multiple Euler-Lagrange systems," IEEE Transactions on Cybernetics, June 2022, 52(6): 4611-4622, .
[5] Zhao X, Han T, Zhan X and Yan H. "Distributed estimator-based fixed-time bipartite consensus of multiple Euler-Lagrange systems over a signed digraph," IEEE Transactions on Circuits and Systems II: Express Briefs, June 2022, 69(6): 2847-2851.
[6] Huang Z, R. Bauer and Pan Y. -J. , "Distributed robust finite-time containment control of Euler-Lagrange systems," 2021 4th IEEE International Conference on Industrial Cyber-Physical Systems (ICPS), 2021, pp. 631-636.
[7] Su H and Zhang L. "Model-independent containment control for dynamic multiple Euler-Lagrange systems with disturbances and uncertainties," IEEE Transactions on Network Science and Engineering, Oct.-Dec. 2021, 8(4): 3443-3452.
[8] Wang L, He H, Zeng Z and Ge M. -F. , "Model-independent formation tracking of multiple Euler–Lagrange systems via bounded Inputs," IEEE Transactions on Cybernetics, May 2021, 51(5): 813-2823, .
[9] Wei B, Xiao F, Fang F and Shi Y."Velocity-free event-triggered control for multiple Euler-Lagrange systems with communication time delays," IEEE Transactions on Automatic Control, Nov. 2021, 66(11): 5599-5605.
[10] Jiang L, Jin Z and Qin Z. "Distributed optimal formation for uncertain Euler-Lagrange systems with collision avoidance," IEEE Transactions on Circuits and Systems II: Express Briefs, Aug. 2022, 69(8): 3415-3419.
[11] Zhou Z. -G., Chen x, Li r, Shi X. -N. and Wen k, "Neuro-adaptive tracking control for uncertain Euler-Lagrange systems with time-varying output constraints and obstacle avoidance," 2020 39th Chinese Control Conference (CCC), 2020, pp. 276-281.
[12] Li t. Development and prospect of power distribution live working robot [J]. Power Supply and Consumption, 2016, 33(11): 43-48.
[13] Xu C. Research on master-slave teleoperation live working robot in distribution network [J]. Machine Tools and Hydraulics, 2019, 47(23): 102-105.
[14] Liu Z. Cable positioning method of live working robot based on laser spot[J]. Application Laser, 2020, 40(5): 140-146, 2020.
[15] Rao Z. Design of 3D environment reconstruction and monitoring system for live working robots [J]. Computer Simulation, 2020, 37(11): 334-338+449..
[16] A. Shakouri and N. Assadian, "Prescribed-time control for perturbed Euler-Lagrange systems with obstacle avoidance," IEEE Transactions on Automatic Control, July 2022, 67(7): 3754-3761.